Convolution Approach for Analysis of Magnetic Forces in Electrical Machines

R. Rothe, M. van der Giet and K. Hameyer

RWTH Aachen University, Inst. of Electrical Machines, Aachen, Germany
E-mail: Richard.Rothe@iem.rwth-aachen.de

***Abstract* — A method for analyzing magnetic forces in electrical machines based on electromagnetic finite element simulation is presented. Sampling of air gap field solution data allows for a Fourier decomposition of magnetic forces and flux densities. A two-dimensional convolution gives insight into the spectral decomposition of forces responsible for acoustic noise, vibration and higher torque harmonics. The approach is applicable to all types of electrical machines that can be modeled in two dimensions. Application examples with a PMSM and an induction machine are presented.**

I. INTRODUCTION

Higher torque harmonics and magnetically excited noise are parasitic effects in electrical machines. They are due to the harmonic forces in the air gap of the machine. Acting on the permeable material of stator and rotor, not only a constant torque but additional torque harmonics are generated, as well as radial forces that excite stator vibrations. These electromagnetic forces can be calculated from the air gap field.

Electromagnetic finite element method (FEM) analyses are used to calculate torques, but also allow for a consideration of local values, such as the magnetic flux density distribution in the air gap. This paper proposes to sample the air gap field solution data of two-dimensional FEM simulations in time and space domain in order to perform a Fourier decomposition and a subsequent two-dimensional periodic convolution of air gap field data. This leads to a geometric addition of partial force components that can be visualized by a space vector diagram. The method has been applied to the radial component of the air gap field for noise analysis purposes [1], and it is generalized in this paper to the convolution of arbitrary sampled two-dimensional data.

In the following the method and its implementation are described. First, some basic Fourier theory is introduced. For an analysis of torque harmonics and noise exciting radial forces, the method is applied to a sinusoidally fed permanent magnet excited synchronous machine (PMSM) and induction machine (IM) model.

II. CONVOLUTION APPROACH

A. Two-dimensional Fourier decomposition and periodic convolution

Since the air gap field and the forces are periodic in time and space, they can be represented by a Fourier series. Let $p : \mathbb{R} \times \mathbb{R} \rightarrow \mathbb{R}$ be continuously differentiable. One has

$$p(\tilde{x},t) = \sum_{n=-\infty}^{\infty} \sum_{m=-\infty}^{\infty} P_{n,m} e^{j(m\Delta r\tilde{x}+n\Delta\omega t)}, \qquad (1)$$

Thanks for your contribution to the success of the EMF 2009 Symposium.

$\Delta\omega = \frac{2\pi}{T}$, $\Delta r = \frac{2\pi}{U}$ with $T, U > 0$ the periods in time and space. The complex Fourier coefficients are determined by

$$P_{n,m} = \frac{1}{U}\frac{1}{T}\int_0^U \int_0^T p(\tilde{x},t) e^{-j(m\Delta r\tilde{x}+n\Delta\omega t)} \mathrm{d}t\mathrm{d}\tilde{x}. \qquad (2)$$

For a Fourier decomposition, many tools process sampled data $y_{n,m}$ by using the discrete Fourier transformation (DFT). The two-dimensional DFT is defined by

$$\mathscr{F}(y_{n,m}) = Y_{n,m} = \sum_{l=0}^{N-1} \sum_{k=0}^{M-1} y_{l,k} e^{-2\pi j(\frac{nl}{N}+\frac{mk}{M})}, \qquad (3)$$

where $n = 0..(N-1)$, $m = 0..(M-1)$. In order to approximate the Fourier series coefficients with Fourier transformation coefficients, a full space-time period U and T is sampled with M and N equidistant steps. The double integral of (2) can be approximated by sums, and after some rearrangements the coefficient approximation results to

$$P_{n,m} \approx \frac{Y_{n,m}}{MN}. \qquad (4)$$

Using Maxwell's stress tensor, tangential force calculation are obtained by the multiplication of normal and tangential air gap field components. The multiplication of values of two sampled data sets $z_{l,k}$ and $z'_{l,k}$ becomes in the frequency mode domain a periodic convolution

$$y_{n,m} = z_{n,m} \cdot z'_{n,m} \Leftrightarrow Y_{n,m} = Z_{n,m} * Z'_{n,m}, \qquad (5)$$

with

$$\begin{aligned} Z_{n,m} * Z'_{n,m} &= \frac{1}{MN} \sum_{l=0}^{N-1} \sum_{k=0}^{M-1} Z_{l,k} \cdot Z'_{n-l,m-k} \\ &\equiv \sum_{l,k} Q_{n,m,l,k} \cdot MN. \end{aligned} \qquad (6)$$

B. Sampling of FEM solution data

In practice, the sampled data are stored into arrays y, z and the two-dimensional DFT is performed by a computer routine. The resulting matrices Y, Z contain the complex Fourier transformation coefficients. Provided that a full space-time period is sampled, the row number n of Y or Z corresponds to the temporal ordinal number and the column number m corresponds to the spacial ordinal number, which is usually called mode or number of pole pair. Each matrix entry $Y_{n,m}$ or $Z_{n,m}$ can be interpreted as a one-dimensional sinusoidal wave. Assuming that matrix z contains sampled data of the radial component of the magnetic flux density in the air gap, a single sinusoidal wave can be expressed by

$$b^r(x,t) = 2\left|\frac{Z_{n,m}}{MN}\right| \frac{\mathrm{Vs}}{\mathrm{m}^2} \cdot \cos(mx + n\Delta\omega t + \arg(\frac{Z_{n,m}}{MN})). \qquad (7)$$

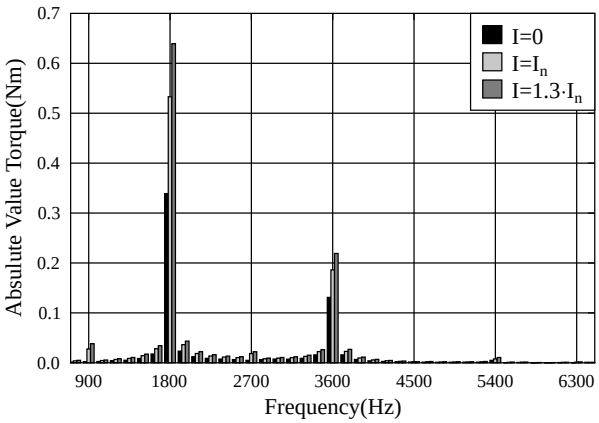

Fig. 1. One-dimensional Fourier decomposition of the output torque[4] of the PMSM model, $n = 4500rpm$, higher harmonics.

This notation is common in analytical considerations of higher air gap field harmonics, [2, 3]. Note that the same harmonic wave is obtained by inversion of the argument of the cosine function, and hence an inversion of the sign of the ordinal numbers. This indicates the symmetry of the DFT transformed matrix

$$Z_{n,m} = Z^*_{-n,-m}. \tag{8}$$

C. Calculation of magnetic forces

Based on the Maxwell stress tensor, the magnetic force vector can be expressed in polar coordinates by

$$\begin{aligned} \boldsymbol{p} &= \boldsymbol{p}^t + \boldsymbol{p}^r \\ &= b^r h^t \, \boldsymbol{e}^t + \frac{1}{2\mu_0}[\,(b^r)^2 - (b^t)^2\,]\,\boldsymbol{e}^r, \end{aligned} \tag{9}$$

where $\boldsymbol{e}^t, \boldsymbol{e}^r$ are polar unit vectors. Discrete data of the radial and tangential air gap field solution $b^r_{n,m}, b^t_{n,m}$ can be obtained by data sampling. Since the DFT is a linear map, a Fourier transformation and a division by $(MN)^2$ according to approximation (4) results to

$$\begin{aligned} \frac{\mathscr{F}(\boldsymbol{p}_{n,m})}{(MN)^2} &= B^r_{n,m} * H^t_{n,m}\, \boldsymbol{e}^t \\ &\quad + \frac{1}{2\mu_0}[B^r_{n,m} * B^r_{n,m} - B^t_{n,m} * B^t_{n,m}]\, \boldsymbol{e}^r. \end{aligned} \tag{10}$$

The tangential component of the air gap field is very small when compared to the radial one. Therefore, (10) is frequently approximated by the simplified Maxwell stress tensor. Then the Fourier series coefficients of the force densities result to

$$\boldsymbol{P}_{n,m} = \frac{\mathscr{F}(\boldsymbol{p}_{n,m})}{MN} = \underbrace{MN \cdot B^r_{n,m} * H^t_{n,m}}_{=P^t_{n,m}}\, \boldsymbol{e}^t + \underbrace{\frac{MN}{2\mu_0} \cdot B^r_{n,m} * B^r_{n,m}}_{=P^r_{n,m}}\, \boldsymbol{e}^r. \tag{11}$$

Two convolution products remain. The tangential forces generate the torque and the radial forces are the main cause for vibration and noise radiation of electrical machines. Normally, the magnetic force density coefficients $P^r_{n,m}$ and $P^t_{n,m}$ are obtained by first multiplying the air gap fields and transferring to the space-time domain. Alternatively, using the convolution allows for a consideration of the summands $Q_{n,m,l,k}$ in (6) as explored in the next section.

D. Visualization with a space vector diagram

Equation (6) shows that the matrix entries of Z are combined by pairs and add up to the total Fourier transformation component $Y_{n,m}$. The geometric addition can be supported by an illustration in the complex plane called space vector diagram, Fig.2. Implemented to a computer routine, partial force Fourier series summands $Q_{n,m,l,k}$ and the associated air gap field pair Fourier components are stored for a subsequent visualization.

In the following the four pole PMSM is considered, Fig.3. A two-dimensional FE simulation reveals that besides the constant torque component, undesired torque harmonics emerge, especially at $f = 1800Hz$, Fig.1. The proposed convolution approach is applied. The radial magnetic flux density component b^r and the tangential magnetic strength component h^t are sampled. The convolution routine transfers the sampled data into the frequency mode domain and generates the space vector diagram of the corresponding tangential Fourier series component $P^t_{24,0}$, Fig.2. The vector chain represents the geometric addition of partial force vectors

$$Q_{l,k} = B^r_{l,k} \cdot H^t_{n-l,m-k}. \tag{12}$$

The involved air gap field harmonic combination pairs are listed in Tab. I. The ordinal numbers $l, k, n-l, m-k$ and the angle have to be added according to (6) and (12). Obviously, only a small number of pairs contribute significantly to the total Fourier series force component $P^t_{24,0}$. The vectors $Q_{l,k}$ are arranged according to their magnitude. Only the first six partial force vectors are depicted. Therefore, a small gap between the vector chain and the total force vector remains.

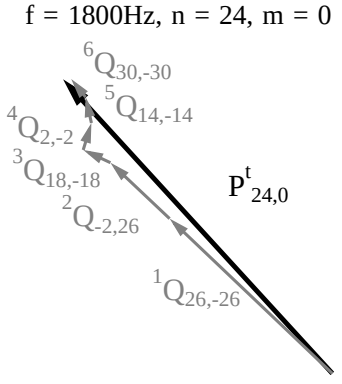

Fig. 2. Space vector diagram, $I = I_n$.

TABLE I. AIR GAP FIELD FOURIER SERIES COMPONENTS FOR $I = I_n$.

Vec	l	k	$2\lvert B^r\rvert$[Vs/m^2]	arg(B^r)[°]	f[Hz]
1	26	-26	0.043677	0.0	1950
2	-2	26	0.027674	46.5	-150
3	18	-18	0.081638	180.0	1350
4	2	-2	1.053000	6.6	150
5	14	-14	0.141511	0.3	1050
6	30	-30	0.048354	180.0	2250
Vec	$n-l$	$m-k$	$2\lvert H^t\rvert$[A/m]	arg(H^t)[°]	f[Hz]
1	-2	26	21793	136.4	-150
2	26	-26	12481	90.1	1950
3	6	18	1559	-25.12	450
4	22	2	113	66.5	1650
5	10	14	795	102.3	750
6	-6	30	2028	51.4	-450

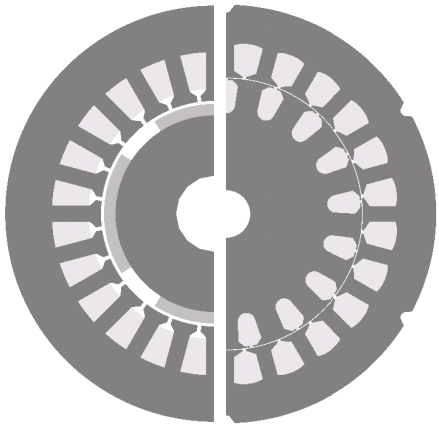

(a) PMSM. (b) IM.

Fig. 3. Scaled cross sections of example machines.

TABLE II. MACHINE DATA.

Machine data	PMSM	IM
Rated power P_n	4 kW	30 kW
Rated speed n_n	4500 rpm	3000 rpm
Rated voltage V_n	230 V	400 V
Rated current I_n	11.2 A	55.6 A
Power factor $cos\varphi_n$	-	0.875
Number of pole pairs p	2	2
Number of stator slots N_S	24	24
PM material	NeFeBo	-
Outer stator diameter D_o	110 mm	232 mm
Air gap sampling radius	29.29mm	85.75mm
Mechanical air gap δ	0.8 mm	0.5 mm
Active length l_{Fe}	120 mm	127 mm

III. APPLICATION TO MACHINE MODELS

A. PMSM model

A rule of thumb for predicting the frequency of the main parasitic torque harmonic is the least common multiple of the number of poles and the number of stator slots, LCM($2p$,N_S)[5]. This harmonic is usually called cogging torque or torque ripple. The considered PMSM has 24 slots, $p = 2$ and the LCM is 24, Tab.II. Since the speed of the machine is $n_n = 4500rpm$, the expected parasitic torque frequency is $f = 1800Hz$. The Fourier decomposition of the toque output of the used FE software[4] meets this prediction, Fig.1.

The cogging component is due to the interaction of the magnetomotive force of the magnets Θ_M and the DC and fundamental component of the stator permeance function Λ, illustrated in Fig. 4, where m is the defined spacial ordinal number, $g_1, g_2, g_3 \in \mathbb{N}$ and $f_1 = 150Hz$ is the frequency of the fundamental air gap field component[5, 3]. The analytically derived and involved air gap field components $b_{M,DC}$ and $b_{M,S}$ as well as the fundamental air gap field component b_1 can be assigned to the decomposition output of the convolution routine by means of their analytically known ordinal numbers. Tab. III lists the involved air gap field convolution pairs of two other simulated operating points $I = 0$ and $I = 1.3 \cdot I_n$ and Fig. 5 shows the geometric addition. The angle between stator field and rotor position remains unchanged.

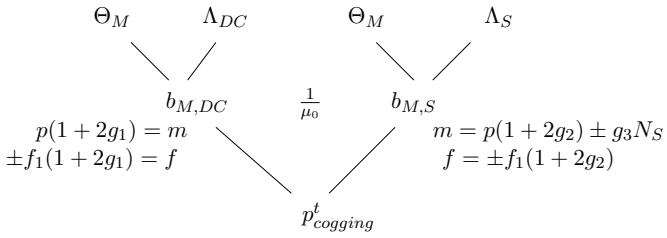

Fig. 4. Excitation of tangential cogging forces.

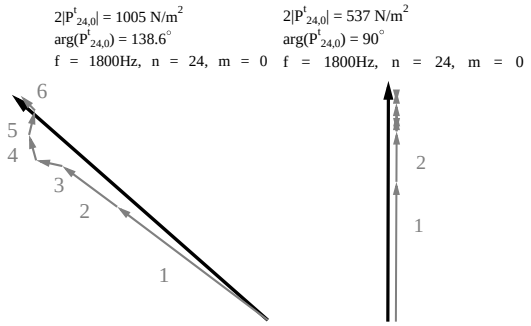

(a) $I = 1.3 \cdot I_n$. (b) $I = 0$.

Fig. 5. Space vector diagrams for $P^t_{24,0}$.

TABLE III.
Air gap field components for (a) $I = 1.3 \cdot I_n$ and (b) $I = 0$.

(a)	l	k	$2\|B^r\|[Vs/m^2]$	$\arg(B^r)[^\circ]$	$f[Hz]$	
1	26	-26	0.043481	0.1	1950.0	$b'_{M,DC}$
2	-2	26	0.032443	53.1	-150.0	$b'_{M,S}$
3	18	-18	0.081647	-179.9	1350.0	$b'_{M,DC}$
4	14	-14	0.141253	0.4	1050.0	$b'_{M,DC}$
5	2	-2	1.055650	8.6	150.0	b_1
6	30	-30	0.048323	180.0	2250.0	$b'_{M,DC}$
(a)	n–l	m–k	$2\|H^t\|[A/m]$	$\arg(H^t)[^\circ]$	$f[Hz]$	
1	-2	26	25561	143.0	-150.0	$b'_{M,S}$
2	26	-26	12416	90.3	1950.0	$b'_{M,DC}$
3	6	18	1938	-12.5	450.0	$b'_{M,S}$
4	10	14	1099	105.0	750.0	$b'_{M,S}$
5	22	2	140	67.9	1650.0	$b'_{M,S}$
6	-6	30	2506	-45.7	-450.0	$b'_{M,DC}$

(b)	l	k	$2\|B^r\|[Vs/m^2]$	$\arg(B^r)[^\circ]$	$f[Hz]$	
1	26	-26	0.043507	-0.2	1950.0	$b_{M,DC}$
2	-2	26	0.018125	-0.0	-150.0	$b_{M,S}$
3	18	-18	0.081554	180.0	1350.0	$b_{M,DC}$
4	-2	2	1.051050	0.0	-150.0	b_1
5	2	-2	1.051050	-0.0	150.0	b_1
6	30	-30	0.048426	179.9	2250.0	$b_{M,DC}$
7	14	-14	0.141744	-0.0	1050.0	$b_{M,DC}$
8	34	-34	0.023964	0.0	2550.0	$b_{M,DC}$
(b)	n–l	m–k	$2\|H^t\|[A/m]$	$\arg(H^t)[^\circ]$	$f[Hz]$	
1	-2	26	14322	90.0	-150.0	$b_{M,S}$
2	26	-26	12388	89.8	1950.0	$b_{M,DC}$
3	6	18	991	-90.0	450.0	$b_{M,S}$
4	26	-2	75	-90.6	1950.0	
5	22	2	59	90.3	1650.0	
6	-6	30	1293	-90.1	-450.0	$b_{M,S}$
7	10	14	388	90.0	750.0	$b_{M,DC}$
8	-10	34	2233	-90.0	-750.0	$b_{M,DC}$

Using a sampling procedure and a DFT, a single sinusoidal wave is always described by two Fourier coefficients together that differ only in the sign of their angle and ordinal numbers according to (8). In Tab. III (b) the fundamental air gap field component b_1 appears two times with inverse values. In fact, both expressions describe the same wave. On the contrary to this, the known analytical derivations employ one expression for one sinusoidal wave by allowing only positive frequencies or positive modes[3].

Compared to the no load case (b), the parasitic force $P^t_{24,0}$ in (a) is increased in magnitude and the angles are distorted, Fig. 5. This can be attributed to the increase of the tangential magnetic strength components H^t generated by the stator currents. Nearly no new partial force vectors $Q_{l,k}$ do appear.

B. IM model

The introduced PMSM model offers an easy handling by sampling one rotor revolution or only one pole pitch revolution. The air gap field of the induction machine revolves asynchronously compared to the rotor. Thus, several rotor revolutions have to be simulated in order to allow for a sampling of a complete time period. If a transient simulation is chosen, additional time steps are necessary to magnetize the rotor until steady state behavior is reached. The considered IM has been simulated for slip $s = 0.008$ and afterwards 62 rotor revolutions have been sampled.

The radial component of the magnetic forces is the main cause for electromagnetically excited vibration and noise radiation. However, the intensity is strongly determined by the distribution of the natural frequencies of the mechanical housing. Also the modes $m = -6...6$ with high mechanical amplifications are of special interest in contrast to the torque, that is solely generated by forces with $m = 0$. The maximum air gap field components and their identification and the maximum forces are listed in Tab. IV. The natural frequencies of the considered IM housing are unknown, therefore the radial example force component is $P^r_{2608,3}$ is singled out for analysis. The partial force components are analogous to (12)

$$Q_{l,k} = \frac{1}{2\mu_0} B^r_{l,k} \cdot B^r_{n-l,m-k}. \tag{13}$$

TABLE IV. Maximum air gap field and magnetic force components ($m = -6...6$), $n \geq 0$.

$2\lvert B^r\rvert[Vs/m^2]$	arg(B^r)[°]	n	m	$f[Hz]$	
0.931856	-47.3	250	-2	100.806	fundam.
0.194274	-15.2	250	22	100.806	stat. slot.
0.176265	-102.3	2358	-19	950.806	rot. slot.
0.166318	20.7	1858	-15	749.193	rot. slot.
0.106786	-161.8	250	-26	100.806	stat. slot.
0.104127	169.9	250	46	100.806	stat. slot.
0.090524	25.4	750	-6	302.419	saturation
$2\lvert P^r\rvert[N/m^2]$	arg(P^r)[°]	n	m	$f[Hz]$	
423884	0.0	0	0	0.0	-
139173	-97.5	500	-4	201.612	-
24806	-168.7	2608	3	1051.612	-
11040	39.8	3092	1	1246.774	-
10510	63.2	1000	4	403.226	-
7924	-35.0	608	-5	245.161	-
5093	136.7	2108	-5	850.000	-
4510	68.5	500	2	201.612	-

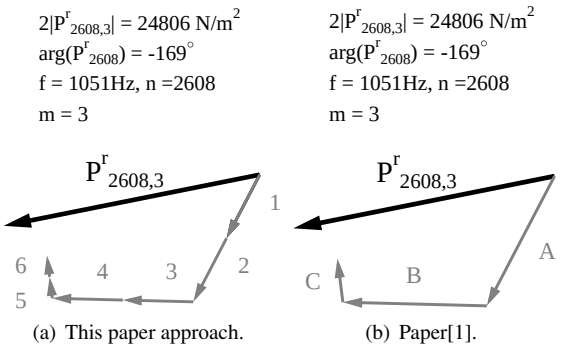

(a) This paper approach. (b) Paper[1].

Fig. 6. Space vector diagrams for $P^r_{2608,3}$.

TABLE V. AIR GAP FIELD COMPONENTS FOR FIG. 6

Vec	l	k	$2\lvert B^r\rvert[Vs/m^2]$	arg(B^r) [°]	$f[Hz]$
1	250	22	0.194274	-15.2	100.806
2	2358	-19	0.176265	-102.3	950.806
3	250	-2	0.931856	-47.3	100.806
4	2358	5	0.036160	-134.2	950.806
5	1858	-15	0.166318	20.7	749.194
6	750	18	0.061925	76.4	302.419
Vec	$n-l$	$m-k$	$2\lvert B^r\rvert[Vs/m^2]$	arg(B^r) [°]	$f[Hz]$
1	2358	-19	0.176265	-102.3	950.806
2	250	22	0.194274	-15.2	100.806
3	2358	5	0.036160	-134.2	950.806
4	250	-2	0.931856	-47.3	100.806
5	750	18	0.061925	76.4	302.419
6	1858	-15	0.166318	20.7	749.194

IV. CONCLUSIONS

The proposed method delivers a deeper insight into the generation of parasitic magnetic forces in rotating electrical machines and may provide additional help for understanding and calculation of higher harmonics beside the analytical approaches. The influence of special design decisions, such as additional holes or notches, that are difficult to calculate analytically, or factors, such as excentricities or certain current shapes, can be analyzed by this way.

Since the output solution of any electromagnetic FEM software is the magnetic vector potential and so the magnetic flux density, an analysis of permeance functions or mmf distributions is not possible. The geometric addition of several air gap field components, excited from different causes, can only be indirectly detected, for instance, by two comparative simulation analyses.

The calculated torque of FEM software is strongly dependent on the mesh refinement in the air gap [5]. This should also be valid for higher air gap field harmonics. Further investigations concerning the influence of the air gap element size and the sample density on the calculated local magnetic forces are to be undertaken. Also a consideration of the neglected tangential air gap fields for the calculation of radial forces is to be taken into account.

The effort and costs for an analysis of the harmonic content of an induction machine model is considerable. Additionally, since a complete time period must be sampled, only discrete operating points are possible. Therefore, the proposed analysis seems especially suitable for synchronous machine models.

REFERENCES

[1] M. van der Giet, R. Rothe, M. Herranz Gracia, and K. Hameyer. Analysis of noise exciting magnetic force waves by means of numerical simulation and a space vector definition. In *18th International Conference on Electrical Machines, ICEM 2008*, pages 1–6, Vilamoura, Portugal, September 2008.

[2] Heinz Jordan. *Geräuscharme Elektromotoren*. W. Girardet, November 1950.

[3] Jacek.F. Gieras, Chong. Wang, and Joseph. Cho Lai. *Noise of Polyphase Electric Motors*. CRC Press Taylor&Francis Group, 2006.

[4] D. van Riesen, C. Monzel, C. Kaehler, C. Schlensok, and G. Henneberger. imoose-an open-source environment for finite-element calculations. *Magnetics, IEEE Transactions on*, 40(2):1390–1393, March 2004.

[5] M. Herranz Gracia. *Methoden zum Entwurf von robusten Stellantrieben unter Berücksichtigung fertigungsbedingter Abweichungen*. Shaker Verlag, Institute of electrical machines, RWTH Aachen, 2009.